**Atmospheric
Chemistry
and Physics
Discussions**

Spatial distribution and seasonal variations of atmospheric sulfur deposition over Northern China

Y. P. Pan, Y. S. Wang, G. Q. Tang, and D. Wu

State Key Laboratory of Atmospheric Boundary Layer Physics and Atmospheric Chemistry (LAPC), Institute of Atmospheric Physics, Chinese Academy of Sciences, Beijing 100029, China

Correspondence to: Y. S. Wang (wys@dq.cern.ac.cn)

ACPD

12, 23645–23677, 2012

Wet and dry deposition of sulfur in Northern China

Y. P. Pan et al.

Title Page

Abstract	Introduction
Conclusions	References
Tables	Figures

|◄ | ►|
◄ | ►

Back | Close

Full Screen / Esc

Printer-friendly Version

Interactive Discussion

Abstract

The increasing anthropogenic emissions of acidic compounds have induced acid deposition accompanied by acidification in the aquatic and terrestrial ecosystems worldwide. However, comprehensive assessment of spatial patterns and long-term trends of acid
5   deposition in China remains a challenge due to a paucity of field-based measurement data, in particular for dry deposition. Here we quantify the sulfur (S) deposition on a regional scale via precipitation, particles and gases during a 3-yr observation campaign at ten selected sites in Northern China. Results show that the total S deposition flux in the target area ranged from 35.0 to 100.7 kg S ha^{-1} yr^{-1}, categorized as high
10 levels compared to those documented in Europe, North America, and East Asia. The ten-site, 3-yr average total S deposition was 64.8 kg S ha^{-1} yr^{-1}, with 32 % attributed to wet deposition, and the rest attributed to dry deposition. Compared with particulate sulfate, gaseous SO$_2$ was the major contributor of dry-deposited S, contributing approximately 49 % to the total flux. Wet deposition of sulfate showed pronounced sea-
15 sonal variations with maximum in summer and minimum in winter, corresponding to precipitation patterns in Northern China. However, the spatial and inter-annual differences in the wet deposition were not significant, which were influenced by the precipitation amount, scavenging ratio and the concentrations of atmospheric S compounds. In contrast, the relatively large dry deposition of SO$_2$ and sulfate during cold season,
20 especially at industrial areas, was reasonably related to the local emissions from home heating. Although seasonal fluctuations were constant, clear spatial differences were observed in the total S deposition flux and higher values were also found in industrial areas with huge emissions of SO$_2$. These findings indicate that human activity has dramatically altered the atmospheric S deposition and thus regional S cycles. To
25 systematically illustrate the potential effects of acidifying deposition on the receiving environment, we calculated the deposition of "potential acidity" that takes into account the microbial transformation of ammonium to nitrate in the ecosystems, resulting in the release of hydrogen ions. The estimated total "acid equivalents" deposition of S and

nitrogen (N) fell within the range of 4.2–11.6 keq ha^{-1} yr^{-1}, with a ten-site, 3-yr mean of 8.4 keq ha^{-1} yr^{-1}. This value is significantly higher than that of other regions in the world and exceeds the critical loads for natural ecosystems in Northern China, thus prompting concerns regarding ecological impacts. The contribution of S to total acid deposition was comparable to that of N at most of sites; however, the importance of S on acidification risks was more pronounced in the industrial sites, highlighting that further SO$_2$ abatement from industrial emissions is still needed. Taking these findings and our previous studies together, a multi-pollutant perspective and joint mitigate strategies to abate SO$_2$ and NH$_3$ simultaneously in the target areas are recommended to protect the natural ecosystems from excess acid deposition caused by anthropogenic emissions.

1 Introduction

Acid deposition, originating largely from man-made emissions of three gaseous pollutants, sulfur dioxide (SO$_2$), nitrogen oxides (NO$_x$) and ammonia (NH$_3$), is a global environmental issue because of its transboundary impacts of the biogeochemical cycles (Rodhe et al., 2002; Flechard et al., 2011). Of concern is the acid deposition that exceeds the critical loads of an ecological system will cause long-term harmful effects, with several deleterious consequences ranging from eutrophication of coastal waters to acidification of lakes, streams, and soils with attendant reductions in species diversity (Reuss et al., 1987; Sickles et al., 2009). With acid deposition behaving as one of the most important environmental issues, decision-makers need to determine which emission controls are needed and to what extent emission reductions will promote ecosystem recovery from acid deposition (Driscoll et al., 2001). To address these concerns, it is essential to gain a quantitative knowledge of acid deposition through monitoring, including SO$_2$, NO$_x$ and NH$_3$ as well as particulate and aqueous forms such as sulfate (SO$_4^{2-}$), nitrate (NO$_3^-$) and ammonium (NH$_4^+$).

In recent decades, the increasing emissions of acidic compounds of sulfur (S) and nitrogen (N) make East Asia one of the most serious acid deposition regions following Europe and North America (Endo et al., 2010; Ayers et al., 2000; Kuribayashi et al., 2012). As one of the most rapidly developing nations in East Asia, China is exposed to acid deposition levels that are amongst the highest around the world (Larssen et al., 2006), with a major contribution from reduced N (NH_x) relative to oxidized N (NO_y) (Larssen et al., 2011) . Under strong environmental pressure, the Chinese government has implemented a variety of control programs including the adjustment of energy structure (Zhao et al., 2009). As a consequence, the increasing trend of annual SO_2 emissions has leveled off since 2006, after which a declining trend has been seen (Lu et al., 2010). In contrast, reactive N emissions by intensive farming and livestock (NH_3) and by traffic and industry (NO_x) are still rising (Liu et al., 2010). These changes in emissions may enhance the N deposition, and thus change the acid deposition pattern in the future. This argument is partially supported by the fact that the ratio of equivalent concentrations of SO_4^{2-} to NO_3^- in precipitation gradually decreased from 5.4 to 1.7 in Beijing (Wang et al., 2012) and from 4.6 to 1.5 in Guangzhou (Fang et al., 2011) during the last few decades. If this trend continues, HNO_3 is expected to play a more important role than H_2SO_4 in determining precipitation acidity in the coming decades. However, the above ratios of larger than unity indicate that precipitation acidity in China was still mainly caused by H_2SO_4, formed via the oxidation of SO_2 (Wang et al., 2012). Although national SO_2 emissions will reduce approximately by 2 % yr^{-1} from 2010 to 2020 if current policy is fully implemented, the exceedance of the critical loads for soil acidification caused by S deposition is still higher than 20 % of the country's territory in 2020 (Zhao et al., 2009). Monitoring information on the S deposition is thus necessary to check whether emission reduction measures are working efficiently (Larssen et al., 2011). Furthermore, enhanced spatial resolution of acid deposition pattern is a key requirement in the application of the critical loads approach to emission control policies (Aherne and Farrell, 2002). Nevertheless, long-term measurement data of acid

deposition are not yet available on a regional scale in China, although the importance of such data has been emphasized previously (Larssen et al., 2006).

Acid deposition monitoring networks have been established in many regions around the world, such as Europe (EMEP), US (CASTNET), Canada (CAPMoN), East Asia (EANET) and Africa (IDAF). In China, acid deposition monitoring conducted routinely across the whole country is lacking. Monitoring of acid rain started in the 1980s, but at few stations only, with a less suitable device setup and incomplete data series (Zhao et al., 1988). Under current national monitoring networks, only general urban air quality parameters and rainwater pH are measured, whereas little has been done involving chemistry determination (Tang et al., 2010). A rapid advance in recent years has been made to investigate the chemical composition responsible for the variations of precipitation pH (Wai et al., 2005; Huang et al., 2008; Sun et al., 2010; Yang et al., 2012; Tsai et al., 2011), but most are limited to a single site/year. Acid deposition can occur by dry deposition of gases and particles and by wet deposition from rain, snow, clouds and fog (Flechard et al., 2011). Thus, data presented only for precipitation chemistry were not enough to accurately assess effects of acid deposition; both the wet and dry deposition flux of S and N must be known. Acid deposition is also spatially and temporally variable (Larssen and Carmichael, 2000), highlighting an urgent requirement to organize an up-to-date national deposition network across the country. Although some sites in Southern China have participated in the EANET, however, the EANET coverage is very sparse in Northern China. To date, fewer measurement results have been focused on N deposition in Northern China (Shen et al., 2009), and field-based data regarding S deposition, in particular dry deposition, are even more scarce.

Northern China is a densely populated and industrialized region with intensive agricultural activities. Associated with the increasing energy use, economic boom and population growth during the past several decades, the substantial emissions of acidic precursors (SO_2, NO_x and NH_3) have intensified the acid deposition problem over the target areas. For example, the precipitation acidity in China remained steady or showed a decreasing trend during the 1990s. After 2000, however, an increasing trend

Wet and dry deposition of sulfur in Northern China

Y. P. Pan et al.

of precipitation acidity was observed at many sites in Northern China (Tang et al., 2010). Besides nutrients, anthropogenic emissions of toxic trace elements and organic pollutants are of concern regarding the related impacts on receiving terrestrial and aquatic ecosystems (Sakata et al., 2006). However, measuring wet and dry deposition of such matters has so far received little attention. To advance our current understanding of their transport and fate from local to regional and global scales, quantitative assessment of atmospheric deposition is required to update with detailed spatial and seasonal descriptions. Therefore, a new monitoring network, including ten sites well distributed within the target area, was set up in late 2007. The focus of the program is to study the wet and dry deposition of important trace species, including carbon, N, S, phosphorus, heavy metals, and polycyclic aromatic hydrocarbons. The network and the resulting scientific research identified that the acidity of precipitation in Northern China generated by H_2SO_4 and HNO_3 was primarily buffered by $CaCO_3$ and NH_3 prior to deposition (Wang et al., 2012). The neutralization of precipitation acidity by alkaline species in the air, however, does not necessarily reduce the potential for acidification of aquatic and terrestrial ecosystems (Galloway et al., 1984). Evidently, a solution of $CaSO_4$ can cause short-term acidification of surface waters as a result of cation-exchange reactions in acid soils (Galloway et al., 1987). Neutralization by NH_3 is also illusory, because the resulting NH_4^+ contributes to acidification of soil and surface water through chemical processes in the soil (Larssen et al., 2006; Driscoll et al., 2001). Therefore, NH_x must be taken into account when quantifying the potential amount of total acid deposition. Additionally, how and to what extent the S and N are contributing to the total acid deposition is largely unknown, though indications of high deposition flux of N have been reported in a companion paper (Pan et al., 2012).

Here we complement the previous study by additionally estimating atmospheric deposition flux of S via precipitation (wet deposition) and as gases and particles (dry deposition) on the basis of a multi-year monitoring at ten selected sites. The objective of this study was to explore the spatial and temporal variations of atmospheric S deposition and its contribution to total acidifying deposition in Northern China. Combined

with N deposition, the unique dataset provides an insight into the total deposition of potential acidity on a regional scale. The knowledge gained from the study provides the up-to-date scientific basis for the validation of emission inventories and atmospheric chemistry models and the crafting of control strategies to reduce their emissions and ecological impacts in the target area.

2 Materials and methods

2.1 Site descriptions

Continuous measurements were carried out during the period from December 2007 to November 2010 at ten sites using the uniform monitoring protocol. Based on the urban geographies, energy structures and ecosystem types, the ten sites were classified into five categories: the two megacity sites located in the Beijing (BJ, 39.96° N, 116.36° E) and Tianjin (TJ, 39.08° N, 117.21° E) downtown areas; two suburban sites 2 km southeast of Cangzhou city (CZ, 38.30° N, 116.87° E) and at Yangfang (YF, 40.15° N, 116.10° E), which is 40 km northwest of Beijing city; three industrial city sites in the center of Baoding city (BD, 38.85° N, 115.50° E), south of Tangshan city (TS, 39.60° N, 118.20° E) and in the coastal Tanggu area (TG, 39.04° N, 117.72° E), which is 30 km east of Tianjin city; two agricultural sites 6 km southwest of Yucheng city (YC, 36.85° N, 116.55° E) and at Luancheng (LC, 37.89° N, 114.69° E), which is 4 km southeast of Shijiazhuang city; and one rural site at Xinglong (XL, 40.38° N, 117.57° E) on Mt. Yan, with an elevation of 960 m a.s.l. Comprehensive descriptions of the stations can be found in Pan et al. (2012).

In order to interpret the geographical distributions of the estimated S deposition, emission patterns of the precursor SO_2 have to be known. Recently, an Asian emission inventory for the year 2006 was developed that includes a database for the study area (Fig. 1a), based on the INTEX-B experiment (Zhang et al., 2009). Hereafter, we refer to this emission inventory as the "INTEX-B". Anthropogenic SO_2 released to the

atmosphere in the INTEX-B was estimated to be 248, 336 and 2281 Gg in Beijing, Tianjin and Hebei province, respectively, making Northern China one of the main "hot spots" of SO_2 emissions in Asia. Power plants and industry are the main sources of SO_2, contributing more than 70 % of the total emissions. Emissions of SO_2 in the target region that are aggregated into grids at a resolution of 30 min × 30 min are shown in Fig. 1b, combined with the 3-yr mean total S deposition that is categorized into five grades and plotted on the maps. Comparisons between depositions and emissions are discussed in Sect. 4.2.

2.2 Wet deposition measurements

Daily rainwater and event-based snow samples were collected using an automatic wet-dry sampler and a clean plastic bucket, respectively. During the 3-yr observation period, a total of 1306 precipitation samples (including rainwater and snow) were collected. All of the precipitation samples were stored, transported, filtered, and analyzed following the prescribed procedure (Pan et al., 2010a). Of the total number of precipitation samples, 16 % were discarded from final analysis due to low volumes (< 20 ml) that did not permit a complete chemical analysis. The concentrations of SO_4^{2-} in the filtrates of the remaining 1107 samples were determined using an ion chromatography system (Model ICS-90, Dionex Corporation, Sunnyvale, CA, USA) and the standard laboratory procedure of the State Key Laboratory of Atmospheric Boundary Layer Physics and Atmospheric Chemistry (Wang et al., 2012). Monthly wet deposition flux of SO_4^{2-} ($_wSO_4^{2-}$, kg S ha^{-1} month^{-1}) was calculated as the product of the volume-weighted mean concentrations of SO_4^{2-} in the precipitation and the precipitation amount measured with the standard rain gauge at each site during the corresponding period. Besides the discarded samples, some light rain events were not sampled due to malfunctions of the automatic rainfall sampler lid (Pan et al., 2010a). These missed samples, accounting for less than 6 % of the annual total depths of precipitation, do not result in significant underestimation of $_wSO_4^{2-}$ observed in the current study.

2.3 Particulate dry deposition measurements

Dry-deposited particles were collected monthly using a surrogate surface made of polyurethane foam (PUF) filter, which was placed in a glass bucket. The sampling and chemical analysis procedures have been detailed previously (Pan et al., 2012) and are only described briefly here. During a rain event, the glass bucket was covered with a lid of the automatic wet-dry collector. After the rainfall ceased, the lid was lifted and rotated to cover the aperture that collected the rainwater. This feature of the automatic sampler is highly useful for simultaneously collecting rainwater and deposited particles with minor mixing of the two. After collection, the content of water-extractable SO_4^{2-} in the PUF filter was determined by the ion chromatography system. Monthly dry deposition flux of particulate SO_4^{2-} ($_pSO_4^{2-}$, $kg\,S\,ha^{-1}\,month^{-1}$) was estimated by dividing the mass of SO_4^{2-} deposited on the PUF filter by the surrogate surface area and the corresponding sampling period.

Measuring dry deposition is known to be much more challenging (Wesely and Hicks, 2000) than that of wet deposition, in terms of measuring the amount and composition of precipitation. Due to gravitational settling, large particles will get trapped easily by PUF-based method used in the study. However, it is difficult to capture fine particles, because impaction and interception with vegetative canopies are the main processes determining their fallout from the air, and such a phenomenon is not reproduced in the design of any standardized artificial collection device (Wesely and Hicks, 2000). Therefore, collection of the dry-deposited particles using surrogate surface method has potential underestimation and the $_pSO_4^{2-}$ measured in the study represents a rather conservative estimation. Despite these precautions, the method can avoid particle bounce and is a cost-effective and convenient way to delineate spatial and temporal information of dry-deposited particles at a variety of locations and over varying time intervals (Pan et al., 2010b).

2.4 Gaseous dry deposition measurements

The inferential method, which combines the measured concentration and a modeled dry deposition velocity (V_d), was used to estimate the gaseous dry deposition flux (Schwede et al., 2011). The method has been used successfully to estimate the dry deposition of reactive N species including NO, NO_2 and NH_3. Gaseous measurements of SO_2 are monthly integrated samples using passive diffusing techniques (Analysts, CNR – Institute of Atmospheric Pollution, Rome, Italy). The ambient SO_2 concentrations were calculated from the SO_4^{2-} levels in the extracts of diffusive samplers corrected by the local temperature and humidity conditions (Costabile et al., 2006). To test the suitability of this sampling technique, the concentration of SO_2 was parallel measured by using a pulsed UV fluorescence analyzer (Model 43i, Thermo-Fisher Scientific, Co., Ltd., Franklin, MA, USA). The results from the passive sampler exposed for one month compare well with the average SO_2 values measured by the in situ continuous active analyzer during the corresponding period, indicating that the passive technique used is reliable for such a study (Wu et al., 2010).

In this study, the hourly V_d of SO_2 and other gases (O_3, NO, NO_2 and NH_3) was simulated using the Models-3/Community Multiscale Air Quality (CMAQ v4.6) system (Byun and Ching, 1999). In its second dry deposition scheme (M3Dry) of CMAQ v4.6, the well-known resistance parameterization for V_d was introduced (Wesely, 1989). Three resistances are considered in this theory: aerodynamic resistance (R_a), quasi-laminar resistance (R_b), and surface or canopy resistance (R_c), among which the R_c is the most difficult one to simulate (Zhang et al., 2008). The V_d is defined as

$$V_d = (R_a + R_b + R_c)^{-1}. \tag{1}$$

This model has proven to be suitable for regional air pollution and acid deposition simulations in China (Zhao et al., 2009). The driving meteorological inputs were provided by the fifth-generation NCAR/Penn State Mesoscale Model (MM5 v3.7). The ambient concentrations of SO_2 measured by passive samplers were multiplied with the average

V_d during the corresponding period to estimate the monthly gaseous dry deposition flux of SO_2 ($_gSO_2$, $kg\,S\,ha^{-1}\,month^{-1}$).

We are however aware that the inferential method is not the best one to clarify gaseous dry deposition flux but an alternative operational tool to compensate for the absence of measured data at regional scales (Flechard et al., 2011). While uncertainties existed in the V_d simulations (Pan et al., 2012), the SO_2 flux is evaluated with the inferential method to give an idea of its contribution to the S budget and thus acid deposition, keeping in mind that it has to be validated with micrometeorological measurements in future field campaigns.

2.5 Statistics

To evaluate the total atmospheric S deposition flux ($_tSO_x$), we compiled the flux data in terms of S from dry-deposited particles, gas and precipitation (including rain and snow) chemistry measurements. Annual $_wSO_4^{2-}$, $_pSO_4^{2-}$, $_gSO_2$, and $_tSO_x$ (generally expressed in the units of $kg\,S\,ha^{-1}\,yr^{-1}$) are integrated from monthly flux datasets.

Total potential acidifying deposition flux (N plus S, hereafter as total acid deposition) is given in mole of protons (H^+) $ha^{-1}\,yr^{-1}$ (converted to $keq\,ha^{-1}\,yr^{-1}$ here) by considering that one mole of total inorganic N ($NH_x + NO_y$) forms one H^+ in the soil and that one mole of $_tSO_x$ ($_wSO_4^{2-} + _pSO_4^{2-} + _gSO_2$) results in two H^+. This calculation accounts for soil microbial transformation of NH_4^+ to NO_3^- with the release of H^+. N deposition data are presented in Pan et al. (2012).

A one-way analysis of variance (ANOVA) and nonparametric tests were performed to examine the significance of differences in the annual flux of S for all ten sites over the three years of the study. A linear regression analysis was used to investigate relationships between precipitation and the wet deposition of SO_4^{2-}. All statistical analyses were conducted using the software SPSS 11.5 (SPSS Inc., Chicago, IL, USA) and Origin 8.0 (Origin Lab Corporation, Northampton, MA, USA).

3 Results

3.1 Wet deposition of sulfate

The mean annual $_w$SO$_4^{2-}$ at the ten sites was relatively high and varied from 14.6 to 24.7 kg S ha^{-1} yr^{-1}, with an average of 19.6 kg S ha^{-1} yr^{-1} during the 3-yr period (Fig. 2). The largest values were observed at the TG site (24.7 kg S ha^{-1} yr^{-1}) followed by the CZ site (22.9 kg S ha^{-1} yr^{-1}). The $_w$SO$_4^{2-}$ was similar for the BJ, TS and YC sites with high values of 21.5, 20.8 and 20.3 kg S ha^{-1} yr^{-1}, respectively. At the YF, BD, and LC sites, the $_w$SO$_4^{2-}$ was moderately large at 19.3, 18.8 and 17.9 kg S ha^{-1} yr^{-1}, respectively. The relatively low flux occurred at the TJ site (15.5 kg S ha^{-1} yr^{-1}), and, as expected, the 3-yr mean values were lowest at the XL site (14.6 kg S ha^{-1} yr^{-1}). However, the differences were not significant ($p > 0.05$) between the sites or the different years, thus indicating the absence of a geographic pattern in the spatial distribution of $_w$SO$_4^{2-}$.

The mean monthly $_w$SO$_4^{2-}$ monitored for the three years ranged from 0 to 6.1 kg S ha^{-1} month^{-1} (Fig. 3a). Seasonal variations of $_w$SO$_4^{2-}$ showed similar trends at each site, with a maximum in summer and minimum in winter. The $_w$SO$_4^{2-}$ was high in June, July, August and September which is in agreement with the rainy season in Northern China. Indeed, the ten-site 3-yr average total $_w$SO$_4^{2-}$ during the summer (June to August) was 11.5 kg S ha^{-1}, which accounted for 58 % of the annual mean $_w$SO$_4^{2-}$. Accordingly, the rainfall amount received was 364 mm during the summer in the study area, which contributed 66 % of the annual precipitation. In contrast, the minimum $_w$SO$_4^{2-}$ level obtained in the winter months was attributable to a low precipitation. In general, a significant linear correlation between the monthly $_w$SO$_4^{2-}$ and precipitation was observed at each site ($0.52 < r^2 < 0.93$, $p < 0.001$); therefore, the precipitation amount is likely to be very important in explaining the seasonal trend of $_w$SO$_4^{2-}$ detected at a given site. Compared with other sites, the $_w$SO$_4^{2-}$ at the YF site showed a different seasonal pattern with relatively high values in March and May. Considering

the precipitation amount between the BJ and YF sites has no significant difference, we suggest that the notably high flux observed in these two months at the YF site is due to local emissions. Additionally, a large standard deviation of $_w\text{SO}_4^{2-}$ was found both in March and May at the YF site. However, such fluctuations can be well explained by the variable depths of precipitation in different years.

3.2 Dry deposition of particulate sulfate

The highest mean annual $_p\text{SO}_4^{2-}$ during the 3-yr period was found at the TS site ($24.8\,\text{kg}\,\text{S}\,\text{ha}^{-1}\,\text{yr}^{-1}$) (Fig. 2), with monthly mean values at this site significantly higher than other sites with the exception of TJ and BD ($p > 0.05$). The second highest result was observed at the TJ site ($19.5\,\text{kg}\,\text{S}\,\text{ha}^{-1}\,\text{yr}^{-1}$), followed by the BD, LC and TG sites, with values of 15.2, 13.4 and $13.1\,\text{kg}\,\text{S}\,\text{ha}^{-1}\,\text{yr}^{-1}$, respectively. However, the monthly mean $_p\text{SO}_4^{2-}$ at these sites was not significantly different ($p > 0.05$). The $_p\text{SO}_4^{2-}$ was comparable for the YC, CZ, BJ and YF sites with values of 10.3, 9.6, 9.3 and $8.4\,\text{kg}\,\text{S}\,\text{ha}^{-1}\,\text{yr}^{-1}$, respectively; differences in the monthly mean values at these sites were also not significant ($p > 0.05$). Annual mean $_p\text{SO}_4^{2-}$ was lowest at the XL site ($4.4\,\text{kg}\,\text{S}\,\text{ha}^{-1}\,\text{yr}^{-1}$), mostly reflecting less emissions surrounding the rural site. The monthly mean flux at this site differed significantly from those at the other sites ($p < 0.05$). In general, annual mean $_p\text{SO}_4^{2-}$ was higher at industrial and urban sites (e.g. TS and TJ) than at suburban and rural sites (e.g. CZ and XL). This observed spatial variation indicates that the annual $_p\text{SO}_4^{2-}$ strongly depends on emissions, increasing with large fossil fuel combustion. Although the LC site is located in an agricultural area, the influence of SO_x plume emitted from industry sources of Shijiazhuang city (the capital of Hebei province) might be the reason why the relatively high annual $_p\text{SO}_4^{2-}$ was observed at the LC site. Compared with TJ and TG, another megacity of BJ and its suburban site YF had relatively low $_p\text{SO}_4^{2-}$, probably reflecting the restriction of SO_x emissions from industry and the relocation of steel industry from BJ to TS.

Title Page

Abstract | Introduction

Conclusions | References

Tables | Figures

◄◄ | ►►

◄ | ►

Back | Close

Full Screen / Esc

Printer-friendly Version

Interactive Discussion

During the 3-yr observation campaign, the mean monthly $_p\text{SO}_4^{2-}$ ranged from 0.1 to 5.1 kg S ha^{-1} month^{-1} (Fig. 3b). At most of the sites, the $_p\text{SO}_4^{2-}$ was higher in the winter and the early spring than in the other seasons, which coincides with the period of home heating in the target areas. This is more pronounced in industrial and urban areas with high population density and thus huge coal consummation even on a relatively small spatial scale (e.g. TJ, TS and BD). In contrast, the lower atmospheric SO_x emissions and efficient wet deposition result in lower $_p\text{SO}_4^{2-}$ during summertime. Different from most sites, the $_p\text{SO}_4^{2-}$ was elevated in June, August and October at the TG, LC and CZ sites, respectively, which is similar to that of $_w\text{SO}_4^{2-}$. These notably high values might be attributable to local sources. In general, the mean monthly $_p\text{SO}_4^{2-}$ was not significantly different ($p > 0.05$) between different years at most of the sites with the exception of BD, BJ, CZ, TG and TS, thus indicating the inter-annual variations of $_p\text{SO}_4^{2-}$. At these five sites, the $_p\text{SO}_4^{2-}$ was found to be lower in 2009 than 2008 and 2010.

3.3 Dry deposition of sulfur dioxide

The mean annual $_g\text{SO}_2$ during the 3-yr period is presented in Fig. 2. The results demonstrated a relatively high $_g\text{SO}_2$ at the industrial TS and urban TJ sites (55.2 and 48.8 kg S ha^{-1} yr^{-1}, respectively); regardless, the difference of monthly means between them was not significant ($p > 0.05$). The mean annual $_g\text{SO}_2$ was high and comparable at the LC, BD, TG, CZ and YC sites with values of 38.9, 37.8, 33.6, 28.9 and 27.3 kg S ha^{-1} yr^{-1}, respectively, and no significantly different monthly mean values were found among the former four sites ($p > 0.05$). The spatial variations of the $_g\text{SO}_2$ were similar to those of $_p\text{SO}_4^{2-}$, both of which illustrated higher flux at certain industrial and urban sites than that of agricultural and rural sites. In general, the monthly mean $_g\text{SO}_2$ was significantly higher at the TJ and TS sites than that of other site with the exception of BD and LC ($p > 0.05$). In contrast, the monthly mean $_g\text{SO}_2$ at the BJ, YF and XL sites was notably lower than other sites ($p < 0.05$), with mean annual values

of 19.5, 18.2 and 16.0 kg S ha^{-1} yr^{-1}, respectively, which is indicative of fewer sources of emissions.

The monthly mean $_g$SO$_2$ during the 3-yr period ranged from 0.4 to 9.0 kg S ha^{-1} month^{-1} (Fig. 3c). Between March and September, the seasonal variation of $_g$SO$_2$ was not distinct at most of the sites, probably because they mainly come from industrial emissions that have less of a seasonal cycle. In contrast, the higher $_g$SO$_2$ values were found during winter and late autumn (November) at the sites of TS, TJ, LC, TG and BD. The notably high $_g$SO$_2$ in cold months suggests an important source, which is related to the fact that extra coal is consumed for home heating.

The year-to-year variations in the annual average $_g$SO$_2$ were comparatively small at each site with the exception of BD, CZ, TG, TJ and TS, which showed significantly lower values in 2010 than in 2009 or 2008 ($p < 0.05$). This is inconsistent with the decreasing trend of SO$_2$ emissions after the year 2006 due to sources control measures implemented in China. Since the gas dry deposition flux is determined by both the concentrations and V_d of the target species, the flux estimates can be significantly different because of differences in the simulated V_d (Pan et al., 2012). We believe the concentration of SO$_2$ may serve as a better index than the flux for tracking the inter-annual trends of emissions. As expected, it was observed that the SO$_2$ concentrations (data not shown) declined year by year in the target area. In general, the ten-site average concentrations of SO$_2$ in 2009 reduced approximately by 18 % compared to 2008 and further declined 36 % from 2009 to 2010, which corresponds well to the decreasing tendencies of SO$_2$ emissions in recent years since 2006. Although differences between the three years are not significant at the 0.05 level at some sites, it is important to point out that $_g$SO$_2$ also tended to decline between 2008/2009 and 2010. Overall, the ten-site average $_g$SO$_2$ in 2010 was 38 % and 45 % lower than in 2008 and 2009. To check whether control measures are working as anticipated, in future work it is intended to investigate the long-term trends of S deposition in the context of evaluating the impacts on ecosystems.

4 Discussion

4.1 Atmospheric total deposition of sulfur in Northern China

Several measurements have been conducted in China in an effort to evaluate the wet and dry deposition of SO_x separately, but few have been performed to determine them simultaneously, especially including dry deposition. To our knowledge, this has not been reported in Northern China before, though previous modeling studies illustrated that S deposition will be enhanced. The mean annual $_tSO_x$ estimated in this study ranged from 35.0 to 100.7 $kg\,S\,ha^{-1}\,yr^{-1}$ over the 3-yr sampling period at the ten sites (Fig. 2). With the exception of BD, LC and TJ, the year-to-year variations in the annual average $_tSO_x$ at most of sites were not significant ($p > 0.05$). Nevertheless, a declining tendency was found for the sites of BD, BJ, LC and TS, while the inter-annual variations at the other sites were more ambiguous. The discrepancy of inter-annual $_tSO_x$ trends between sites is reasonable, because the year-to-year variations of $_wSO_4^{2-}$ and $_pSO_4^{2-}$ do not show any marked trend. As presented in Fig. 3d, the monthly mean $_tSO_x$ during the 3-yr period ranged from 1.4 to 11.7 $kg\,S\,ha^{-1}\,month^{-1}$; however, the seasonal trends at most sites did not significantly differ, indicating that the $_tSO_x$ was constant throughout the entire year as a result of opposite seasonal trends of wet vs. dry deposition of S at a given site.

The spatial variation of $_tSO_x$ was in agreement with that of gaseous and particulate dry deposition; the values at the LC, BD, TG, CZ and YC sites were higher than those at the BJ, YF and XL sites and lower than those at the TS and TJ sites. The overall mean $_tSO_x$ in Northern China was 64.8 $kg\,S\,ha^{-1}\,yr^{-1}$ during the 3-yr period, which was approximately 4 to 10 times that observed by CASTNET, EMEP and EANET with values of 6.2, 6.2 and 17.6 $kg\,S\,ha^{-1}\,yr^{-1}$, respectively (Endo et al., 2010). Since most sites in these abroad networks were located in less polluted areas, perhaps using the rural XL site as the critical baseline of the heavily S deposition would be more reflective of the effects of human-induced emissions in the target areas. Even then, the $_tSO_x$ at

the site XL ($35.0\,\text{kg}\,\text{S}\,\text{ha}^{-1}\,\text{yr}^{-1}$) was approximately 2 to 5 times that observed by the above monitoring networks, indicating a high level of S deposition in Northern China as a result of huge SO_2 emissions.

In addition, the total S deposition at the XL site was likely underestimated because fog water is an important atmospheric deposition process in mountainous forest areas but not measured in this study; however, the rate of S deposition through fog, wet and dry deposition to high-elevation forests in the US ($16.3\,\text{kg}\,\text{S}\,\text{ha}^{-1}\,\text{yr}^{-1}$) (Miller et al., 1993) and Japan (16.7–$27.7\,\text{kg}\,\text{S}\,\text{ha}^{-1}\,\text{yr}^{-1}$) (Shimadera et al., 2012) was still significantly lower than the present study. In the future, north-central and eastern China is expected to receive the most S depositions by the CMAQ simulations, attributed mainly to high densities of energy consumption and emissions (Zhao et al., 2009). Besides the present field-evidence data, the predicted spatial pattern of S deposition in China can be further confirmed by the fact that the total airborne SO_x input into the farmland in Jiangxi, China is estimated to be $103\,\text{kg}\,\text{S}\,\text{ha}^{-1}\,\text{yr}^{-1}$ (Wang et al., 2003), which is greater than the results found for the agricultural sites of LC and YC (70.2 and $58.0\,\text{kg}\,\text{S}\,\text{ha}^{-1}\,\text{yr}^{-1}$, respectively) in this study. Therefore, the sufficiently high S deposition in vast areas in China suggests the need for integrated assessment of the effects of excess S deposition on different ecosystems.

4.2 Anthropogenic imprints on sulfur deposition in Northern China

In order to address the above concerns and thus help policy-makers mitigate S deposition, the sources of SO_2 have to be known. Evidently, several points may support the significant influences of human activity on the S deposition in the target areas. First, the relatively high $_t SO_x$ was found at the sites of TS, TJ, BD and LC, which is surrounded by large SO_2 emissions sources (Fig. 1b). Although the discrepancy between emissions and depositions observed at the sites of BJ and YC may be attributable to the overestimations in current gridded inventories of INTEX-B, the relatively low $_t SO_x$ at the XL and YF sites indicated fewer anthropogenic emissions. Overall, the $_t SO_x$ tends to

increase in relation to human-induced SO_2 emissions and a spatial pattern is identified here.

Second, it has been noted elsewhere that dry deposition of trace species is dominated by local emissions (Balestrini et al., 2000); the idea was verified here. The sites that had significantly higher dry deposition of S were mostly located in the industrial areas such as TS, TJ and BD, or influenced by the industry plume, in particular LC. Although the wet deposition, when considered in terms of annual flux, showed no significant differences between sites, the high local emissions near the sites had apparent effect on the precipitation flux. With the aim of identifying potential factors influencing the spatial pattern of wet depositions, we performed a statistical analysis of data from the 3-yr period following previous studies (Sakata et al., 2006). The results illustrated a moderate linear relationship between the annual $_wSO_4^{2-}$ and the corresponding precipitation amounts ($p < 0.05$). However, only 23 % of the variance of the $_wSO_4^{2-}$ ($r^2 = 0.23$) was explained by the annual precipitation (Fig. 4), implying marked differences in the scavenging ratio and the atmospheric concentrations of SO_x across Northern China, which is similar to that of NH_4^+ (Pan et al., 2012). Specifically, the annual $_wSO_4^{2-}$ at the sites of BD, LC and TG tends to be much higher than that expected from the precipitation amount, which is indicative of large contribution from man-made emissions. Such a contribution also resulted in peak values of $_wSO_4^{2-}$ in September and October at the CZ site (Fig. 3a), and in March and May at the YF site, as discussed in Sect. 3.1.

Third, in dry deposition the seasonal trend of $_gSO_2$ and $_pSO_4^{2-}$ was ostensibly linked to local anthropogenic emissions. The relatively high values of dry deposition in cold months clearly suggested the importance of emissions from coal combustion sources for the total S deposition. In winter, the SO_2 concentration from passive samples was about 3 times that in summer, explained as due to an additionally higher contribution from coal burning during home heating periods. Furthermore, significant fluctuations of $_gSO_2$ between most of industrial sites in late autumn and winter, in association with SO_2 concentrations, reflected the differences in the emission strength.

4.3 Contribution of different pathways to total S deposition flux

The $_g SO_2$ was the major contributor to $_t SO_x$ at most sites, and the contribution ranged from 39 % (BJ) to 58 % (TJ), averaging 49 %. Only at the megacity BJ and its suburban site YF was the contribution of $_g SO_2$ less than that of $_w SO_4^{2-}$. In contrast, the contribution of S deposition through $_g SO_2$ was larger than 50 % at the sites of TJ, BD, TS and LC, which is due in part to the proximity of the sites to high emission areas. The mean annual $_g SO_2$ in this study reached 32.4 kg S ha^{-1} yr^{-1}. This result is much higher than that modeled in South Korea (3.5 kg S ha^{-1} yr^{-1}) (Park and Lee, 2003) and Japan (approximately 3.1 kg S ha^{-1} yr^{-1}) (Endo et al., 2010), and values determined over a coniferous canopy in The Netherlands (4.3 kg S ha^{-1} yr^{-1}) using the aerodynamic gradient technique (Wyers and Duyzer, 1997). Given the influence of local SO_2 emissions from intensive industrialization, it is not surprising that the $_g SO_2$ at the TJ and TS sites reached 48.8 and 55.2 kg S ha^{-1} yr^{-1}, respectively. However, these values are much lower than the result from the farmland in Jiangxi, China (79.6 kg S ha^{-1} yr^{-1}), which could be attributable to the influence of SO_2 emissions from anthropogenic sources (Wang et al., 2003). The influence of SO_2 emissions could also explain why the sites BD and LC had a higher $_g SO_2$ value than the other agricultural, urban and rural locations, including YC, BJ, YF and XL ($p < 0.05$).

The $_w SO_4^{2-}$ contributed 19–43 % to $_t SO_x$ with a ten-site, 3-yr mean of 32 %, which was 17 % lower than that of $_g SO_2$. Of note is the fact that the contribution of $_w SO_4^{2-}$ to $_t SO_x$ exceeds that of $_g SO_2$ at the BJ and YF sites, implying that precipitation was the largest contributor to the total S deposition. The ten-site average $_w SO_4^{2-}$ in Northern China was 19.6 kg S ha^{-1} yr^{-1} from 2008 to 2010. This result is comparable to the values from Jiangxi (17.2 kg S ha^{-1} yr^{-1}) (Wang et al., 2003) and the other Chinese subtropical forest catchment (14.4–30.4 kg S ha^{-1} yr^{-1}) (Larssen et al., 2011), but much higher than the modeled $_w SO_4^{2-}$ in Hong Kong (9.6 kg S ha^{-1} yr^{-1}) (Ayers and

Title Page

Abstract | Introduction

Conclusions | References

Tables | Figures

◄ | ►

Back | Close

Full Screen / Esc

Printer-friendly Version

Interactive Discussion

Wet and dry deposition of sulfur in Northern China

Y. P. Pan et al.

Yeung, 1996), and the values (3.8–$11.2\,kg\,S\,ha^{-1}\,yr^{-1}$) reported by CASTNET, EMEP and EANET (Endo et al., 2010).

Compared with $_g SO_2$ and $_w SO_4^{2-}$, the proportion of $_p SO_4^{2-}$ to $_t SO_x$ was relatively small, falling in the range of 13–25 % with an average of 19 %. It is worth noting that the contribution of $_p SO_4^{2-}$ to $_t SO_x$ exceeds that of $_w SO_4^{2-}$ at the TJ and TS sites, thus reflecting the intense perturbation of the atmospheric particulate SO_4^{2-} by anthropogenic activities. The mean annual $_p SO_4^{2-}$ ranged from 4.4 to $24.8\,kg\,S\,ha^{-1}\,yr^{-1}$ with a mean of $12.8\,kg\,S\,ha^{-1}\,yr^{-1}$ during the 3-yr period. This value is comparable to that from the Jiangxi, China ($6.7\,kg\,S\,ha^{-1}\,yr^{-1}$) (Wang et al., 2003) and Chicago, US (3.7–$14.6\,kg\,S\,ha^{-1}\,yr^{-1}$) estimated using a dry deposition velocity model (Lestari et al., 2003) but much higher than the $_p SO_4^{2-}$ modeled in South Korea ($0.6\,kg\,S\,ha^{-1}\,yr^{-1}$) (Park and Lee, 2003) and results determined over a coniferous canopy in The Netherlands ($1.8\,kg\,S\,ha^{-1}\,yr^{-1}$) using the aerodynamic gradient technique (Wyers and Duyzer, 1997), and values from Japan (approximately $3.2\,kg\,S\,ha^{-1}\,yr^{-1}$), which were estimated using the inferential method (Endo et al., 2010).

The current measurements obtained in this study allowed us to systematically evaluate the S deposition via different pathways in Northern China, whereas previous studies only focused on either the wet or the dry deposition. Overall, precipitation, particulate and gas dry deposition respectively accounted for 32 %, 19 % and 49 % of the total S deposition in Northern China. The S deposition pattern was similar to that of N deposition, which showed the largest contribution of gas (50 %), followed by precipitation (40 %) and particles (10 %) (Pan et al., 2012). However, the contribution of precipitation to total S deposition was 8 % lower compared with that of N deposition, whereas the contribution of particulate dry deposition to total S deposition was two times that of N deposition. These differences probably indicated that the particulate dry deposition played a more important role in the S deposition than that of N. One such study conducted in South China also showed that the largest input of atmospheric S into the farmland ecosystem was gas (77 %), followed by rainwater (17 %) and particles

(6 %) (Wang et al., 2003). The relatively high SO_2 dry deposition and its role played in the total S deposition probably reflected heavy SO_2 pollution in China emitted from anthropogenic sources.

4.4 Acid deposition in Northern China and its implications

Acid deposition of SO_4^{2-} has been widely documented due to concerns about the impacts of this deposited compound on the acidity of the environment. Besides SO_4^{2-}, however, NO_3^-, NH_4^+, NO_x, NH_3, and SO_2 also contribute to the acidification of ecosystems. Thus, there is a necessity for quantification of total acid deposition to inform the control strategies for atmospheric pollution. Specifically, the total S deposition in this study ranged from 2.2 to 6.3 keq ha^{-1} yr^{-1} with a ten-site mean of 4.1 keq ha^{-1} yr^{-1} (Fig. 5), which is much higher than the critical loads (< 2.0 keq ha^{-1} yr^{-1}) for acidification in most areas of Northern China (Zhao et al., 2009). Since the critical loads are defined as the indicator of ecosystem sensitivity, the total S deposition exceeding the critical loads indicated that harmful ecological effects will happen or may have already occurred (Larssen et al., 2011).

With the aim of determining the contribution of acidifying species into the environment, the total deposition of "acid equivalents" of S and N was estimated by summing the wet and the particulate dry deposition flux of SO_4^{2-}, NO_3^-, NO_2^- and NH_4^+, and the estimated dry deposition flux of SO_2, NO_2, NO and NH_3. Taking N deposition data from our companion paper into account (Pan et al., 2012), the total acid deposition ranged from 4.2 to 11.6 keq ha^{-1} yr^{-1} with a ten-site mean of 8.4 keq ha^{-1} yr^{-1} (Fig. 5) falling in the range of 1.9–13 keq ha^{-1} yr^{-1} in forested catchments in Southern China (Larssen et al., 2011). However, acid deposition in the study is roughly 10 times the results in Malaysia (0.3–0.5 keq ha^{-1} yr^{-1}) (Ayers et al., 2000), and is also much higher than previous estimates from high-elevation forests in the US (2.2 keq ha^{-1} yr^{-1}) (Miller et al., 1993) and the values (0.8–1.9 keq ha^{-1} yr^{-1}) reported by CASTNET, EMEP and EANET (Endo et al., 2010). The acid deposition value in Northern China is sufficiently

Wet and dry deposition of sulfur in Northern China

Y. P. Pan et al.

Title Page

Abstract	Introduction
Conclusions	References
Tables	Figures

◄◄   ►►

◄   ►

Back   Close

Full Screen / Esc

Printer-friendly Version

Interactive Discussion

high so as to suggest the need for integrated assessment of acidic deposition and potential environmental consequences in the region (Zhao et al., 2009; Larssen et al., 2011; Hao et al., 2001).

The atmospheric deposition of S has been of interest for many years; however, the importance of N on acidification risks is clearly demonstrated in our study if the acidification effect of N is combined with that of S. As illustrated in Fig. 5, the contribution of N to acid deposition was higher than that of S at most of sites with the exception of TS, TJ, BD and XL. The relatively high contribution of S to total acid deposition at these four sites highlights that further SO_2 abatement in industrial regions is still needed, further considering the large S deposition in rural areas of Northern China. It should be noted that the contribution of S to total acid deposition was almost in the same range as that of N at most of sites (Fig. 5), with the exception of the BJ, TG, YC and LC sites where NH_3 deposition is large (Pan et al., 2012). Thus, to mitigate acid deposition and its potential impacts on receiving ecosystems, a multi-pollutant perspective and joint control strategies to abate SO_2 and NH_3 simultaneously in the target areas are recommended (Zhao et al., 2009).

5 Conclusions

The proportion of cities in Northern China experiencing acid rain (pH < 5.6) has increased during recent years, arousing great concerns about the effects of the deposited material on the acidity of the environment. Compared with precipitation, atmospheric dry deposition of acidifying species is suggested to be an important process determining their lifetime in air and their input to various ecosystems. Furthermore, the acid deposition is likely to be much greater in Northern China because of large emissions of reactive N and S species. However, few studies have been carried out over the target area to simultaneously quantify both the wet and the dry deposition. Additionally, the contribution of S to acid deposition remains unclear, though N deposition has been reported in our companion paper (Pan et al., 2012). These are, to our knowledge, the

first detailed measurements of S deposition via precipitation (wet deposition) and as particles and gases (dry deposition) in Northern China. The major findings are as follows.

1. The seasonal variations were clear in the $_wSO_4^{2-}$ with higher values observed in summer than other seasons, which corresponded with the seasonal trend of precipitation in Northern China. The relatively large $_gSO_2$ and $_pSO_4^{2-}$ during cold season were reasonably related to the local emissions from home heating.

2. Both the $_gSO_2$ and $_pSO_4^{2-}$ showed spatial variations, with significant values observed at sites close to industrial emissions. However, the spatial differences in the wet deposition were not significant between the ten sites or in the different years, which was influenced by the precipitation amount, scavenging ratio and the concentrations of S compounds in the air.

3. Although the concentrations of SO_2 decreased year by year, which is line with the declining trend of the SO_2 emissions since 2006, the inter-annual trends of S deposition were more ambiguous, highlighting that the future study should focus on long-term monitoring of S deposition in the context of evaluating the efficiency of control measures and impacts on ecosystems.

4. The seasonal fluctuation of $_tSO_x$ was constant while the spatial variations were similar to that of dry deposition, which has strong emission dependence. The $_gSO_2$ contributed the most (49 %) to the $_tSO_x$ (64.8 kg S ha^{-1} yr^{-1}) among the three deposition pathways in Northern China. On the other hand, the $_wSO_4^{2-}$ and $_pSO_4^{2-}$ respectively accounted for 32 % and 19 % to $_tSO_x$.

This unique dataset provides field-based evidence that the $_tSO_x$ in Northern China is significantly higher than other regions of the world. The results also indicated that dry deposition is an important deposition process in the target areas and wet deposition cannot be used alone to determine the $_tSO_x$. If the acidification effect of S is combined with that of N, the estimated acid deposition exceeds the critical loads for natural

ecosystems, thus prompting concerns regarding ecological impacts. The contribution of S to total acid deposition is on the same level as that of N at most of sites; however, the acidification risks of S were more pronounced in the industrial areas. To mitigate acid deposition in the target areas, priority should be given to strategies for abating

5　SO_2 and NH_3 simultaneously.

References

Aherne, J. and Farrell, E. P.: Deposition of sulphur, nitrogen and acidity in precipitation over Ireland: chemistry, spatial distribution and long-term trends, Atmos. Environ., 36, 1379–1389,

15　doi:10.1016/S1352-2310(01)00507-6, 2002.

Ayers, G. P. and Yeung, K. K.: Acid deposition in Hong Kong, Atmos. Environ., 30, 1581–1587, doi:10.1016/1352-2310(95)00454-8, 1996.

Ayers, G. P., Peng, L. C., Fook, L. S., Kong, C. W., Gillett, R. W., and Manins, P. C.: Atmospheric concentrations and deposition of oxidised sulfur and nitrogen species at Petaling

20　Jaya, Malaysia, 1993–1998, Tellus B, 52, 60–73, doi:10.1034/j.1600-0889.2000.00043.x, 2000.

Balestrini, R., Galli, L., and Tartari, G.: Wet and dry atmospheric deposition at prealpine and alpine sites in Northern Italy, Atmos. Environ., 34, 1455–1470, doi:10.1016/s1352-2310(99)00404-5, 2000.

25　Byun, D. W. and Ching, J. K. S.: Science algorithms of the EPA Models-3 community multiscale air quality (CMAQ) modeling system; Report EPA/600/R-99/030; US Environmental Protection Agency, Research Triangle Park, NC, 1999.

Wet and dry deposition of sulfur in Northern China

Y. P. Pan et al.

Title Page

Abstract	Introduction
Conclusions	References
Tables	Figures

|◄ | ►|

◄ | ►

Back | Close

Full Screen / Esc

Printer-friendly Version

Interactive Discussion

Costabile, F., Bertoni, G., Desantis, F., Wang, F., Weimin, H., Fenglei, L., and Allegrini, I.: A preliminary assessment of major air pollutants in the city of Suzhou, China, Atmos. Environ., 40, 6380–6395, doi:10.1016/j.atmosenv.2006.05.056, 2006.

Driscoll, C. T., Lawrence, G. B., Bulger, A. J., Butler, T. J., Cronan, C. S., Eagar, C., Lambert, K. F., Likens, G. E., Stoddard, J. L., and Weathers, K. C.: Acidic deposition in the Northeastern United States: sources and inputs, ecosystem effects, and management strategies, Bioscience, 51, 180–198, doi:10.1641/0006-3568(2001)051[0180:ADITNU]2.0.CO;2, 2001.

Endo, T., Yagoh, H., Sato, K., Matsuda, K., Hayashi, K., Noguchi, I., and Sawada, K.: Regional characteristics of dry deposition of sulfur and nitrogen compounds at EANET sites in Japan from 2003 to 2008, Atmos. Environ., 45, 1259–1267 doi:10.1016/j.atmosenv.2010.12.003, 2010.

Fang, Y. T., Koba, K., Wang, X. M., Wen, D. Z., Li, J., Takebayashi, Y., Liu, X. Y., and Yoh, M.: Anthropogenic imprints on nitrogen and oxygen isotopic composition of precipitation nitrate in a nitrogen-polluted city in southern China, Atmos. Chem. Phys., 11, 1313–1325, doi:10.5194/acp-11-1313-2011, 2011.

Flechard, C. R., Nemitz, E., Smith, R. I., Fowler, D., Vermeulen, A. T., Bleeker, A., Erisman, J. W., Simpson, D., Zhang, L., Tang, Y. S., and Sutton, M. A.: Dry deposition of reactive nitrogen to European ecosystems: a comparison of inferential models across the NitroEurope network, Atmos. Chem. Phys., 11, 2703–2728, doi:10.5194/acp-11-2703-2011, 2011.

Galloway, J. N., Likens, G. E., and Hawley, M. E.: Acid precipitation: natural versus anthropogenic components, Science, 226, 829–831, doi:10.1126/science.226.4676.829, 1984.

Galloway, J. N., Zhao, D. W., Xiong, J. L., and Likens, G. E.: Acid rain: China, United States, and a remote area, Science, 236, 1559–1562, doi:10.1126/science.236.4808.1559, 1987.

Hao, J., Duan, L., Zhou, X., and Fu, L.: Application of a LRT model to acid rain control in China, Environ. Sci. Technol., 35, 3407–3415, doi:10.1021/es001888u, 2001.

Huang, K., Zhuang, G., Xu, C., Wang, Y., and Tang, A.: The chemistry of the severe acidic precipitation in Shanghai, China, Atmos. Res., 89, 149–160, doi:10.1016/j.atmosres.2008.01.006, 2008.

Kuribayashi, M., Ohara, T., Morino, Y., Uno, I., Kurokawa, J., and Hara, H.: Long-term trends of sulfur deposition in East Asia during 1981–2005, Atmos. Environ., 59, 461–475, doi:10.1016/j.atmosenv.2012.04.060, 2012.

Larssen, T. and Carmichael, G. R.: Acid rain and acidification in China: the importance of base cation deposition, Environ. Pollut., 110, 89–102, doi:10.1016/s0269-7491(99)00279-1, 2000.

Wet and dry deposition of sulfur in Northern China

Y. P. Pan et al.

Title Page

Abstract	Introduction
Conclusions	References
Tables	Figures

◀◀   ▶▶

◀   ▶

Back   Close

Full Screen / Esc

Printer-friendly Version

Interactive Discussion

Larssen, T., Lydersen, E., Tang, D., He, Y., Gao, J., Liu, H., Duan, L., Seip, H. M., Vogt, R. D., and Mulder, J.: Acid rain in China, Environ. Sci. Technol., 40, 418–425, doi:10.1021/es0626133, 2006.

Larssen, T., Duan, L., and Mulder, J.: Deposition and leaching of sulfur, nitrogen and calcium in four forested catchments in China: implications for acidification, Environ. Sci. Technol., 45, 1192–1198, doi:10.1021/es103426p, 2011.

Lestari, P., Oskouie, A. K., and Noll, K. E.: Size distribution and dry deposition of particulate mass, sulfate and nitrate in an urban area, Atmos. Environ., 37, 2507–2516, doi:10.1016/s1352-2310(03)00151-1, 2003.

Liu, X. J., Duan, L., Mo, J. M., Du, E., Shen, J. L., Lu, X. K., Zhang, Y., Zhou, X. B., He, C. E., and Zhang, F. S.: Nitrogen deposition and its ecological impact in China: an overview, Environ. Pollut., 155, 2251–2264, doi:10.1016/j.envpol.2010.08.002, 2010.

Lu, Z., Streets, D. G., Zhang, Q., Wang, S., Carmichael, G. R., Cheng, Y. F., Wei, C., Chin, M., Diehl, T., and Tan, Q.: Sulfur dioxide emissions in China and sulfur trends in East Asia since 2000, Atmos. Chem. Phys., 10, 6311–6331, doi:10.5194/acp-10-6311-2010, 2010.

Miller, E. K., Panek, J. A., Friedland, A. J., Kadlecek, J., and Mohnen, V. A.: Atmospheric deposition to a high-elevation forest at Whiteface Mountain, New York, USA, Tellus B, 45, 209–227, doi:10.1034/j.1600-0889.1993.t01-2-00001.x, 1993.

Pan, Y. P., Wang, Y. S., Xin, J. Y., Tang, G. Q., Song, T., Wang, Y. H., Li, X. R., and Wu, F. K.: Study on dissolved organic carbon in precipitation in Northern China, Atmos. Environ., 44, 2350–2357, doi:10.1016/j.atmosenv.2010.03.033, 2010a.

Pan, Y. P., Wang, Y. S., Yang, Y. J., Wu, D., Xin, J. Y., and Fan, W. Y.: Determination of trace metals in atmospheric dry deposition with a heavy matrix of PUF by inductively coupled plasma mass spectroscopy after microwave digestion, Environ. Sci., 31, 553–559, 2010b (in Chinese).

Pan, Y. P., Wang, Y. S., Tang, G. Q., and Wu, D.: Wet and dry deposition of atmospheric nitrogen at ten sites in Northern China, Atmos. Chem. Phys., 12, 6515–6535, doi:10.5194/acp-12-6515-2012, 2012.

Park, S. U. and Lee, E. H.: Long-range transport contribution to dry deposition of acid pollutants in South Korea, Atmos. Environ., 37, 3967–3980, doi:10.1016/S1352-2310(03)00470-9, 2003.

Reuss, J. O., Cosby, B. J., and Wright, R. F.: Chemical processes governing soil and water acidification, Nature, 329, 27–32, doi:10.1038/329027a0, 1987.

Wet and dry deposition of sulfur in Northern China

Y. P. Pan et al.

Title Page

Abstract	Introduction
Conclusions	References
Tables	Figures

◄◄   ►►

◄   ►

Back   Close

Full Screen / Esc

Printer-friendly Version

Interactive Discussion

Rodhe, H., Dentener, F., and Schulz, M.: The global distribution of acidifying wet deposition, Environ. Sci. Technol., 36, 4382–4388, doi:10.1021/es020057g, 2002.

Sakata, M., Marumoto, K., Narukawa, M., and Asakura, K.: Regional variations in wet and dry deposition fluxes of trace elements in Japan, Atmos. Environ., 40, 521–531, doi:10.1016/j.atmosenv.2005.09.066, 2006.

Schwede, D., Zhang, L., Vet, R., and Lear, G.: An intercomparison of the deposition models used in the CASTNET and CAPMoN networks, Atmos. Environ., 45, 1337–1346 doi:10.1016/j.atmosenv.2010.11.050, 2011.

Shen, J. L., Tang, A. H., Liu, X. J., Fangmeier, A., Goulding, K. T. W., and Zhang, F. S.: High concentrations and dry deposition of reactive nitrogen species at two sites in the North China Plain, Environ. Pollut., 157, 3106–3113, doi:10.1016/j.envpol.2009.05.016, 2009.

Shimadera, H., Kondo, A., Shrestha, K. L., Kaga, A., and Inoue, Y.: Annual sulfur deposition through fog, wet and dry deposition in the Kinki Region of Japan, Atmos. Environ., 45, 6299–6308, doi:10.1016/j.atmosenv.2011.08.055, 2012.

Sickles II, J. E., Shadwick, D. S., Kilaru, J. V., and Grimm, J. W.: Errors in representing regional acid deposition with spatially sparse monitoring: case studies of the Eastern US using model predictions, Atmos. Environ., 43, 2855–2861, doi:10.1016/j.atmosenv.2009.03.018, 2009.

Sun, M., Wang, Y., Wang, T., Fan, S., Wang, W., Li, P., Guo, J., and Li, Y.: Cloud and the corresponding precipitation chemistry in South China: water-soluble components and pollution transport, J. Geophys. Res., 115, D22303, doi:10.1029/2010JD014315, 2010.

Tang, J., Xu, X. B., Ba, J., and Wang, S. F.: Trends of the precipitation acidity over China during 1992–2006, Chinese. Sci. Bull., 55, 1800–1807, doi:10.1007/s11434-009-3618-1, 2010.

Tsai, Y. I., Hsieh, L. Y., Kuo, S. C., Chen, C. L., and Wu, P. L.: Seasonal and rainfall-type variations in inorganic ions and dicarboxylic acids and acidity of wet deposition samples collected from subtropical East Asia, Atmos. Environ., 45, 3535–3547, doi:10.1016/j.atmosenv.2011.04.001, 2011.

Wai, K. M., Tanner, P. A., and Tam, C. W. F.: 2-year study of chemical composition of bulk deposition in a South China coastal city: comparison with East Asian cities, Environ. Sci. Technol., 39, 6542–6547, doi:10.1021/es048897d, 2005.

Wang, T. J., Zhang, Y., Zhang, M., Hu, Z. Y., Xu, C. K., and Zhao, Y. W.: Atmoshperic sulfur deposition and the sulfur nutrition of crops at an agricututral site in Jiangxi province of China, Tellus B, 55, 893–900, doi:10.1046/j.1435-6935.2003.00076.x, 2003.

Wet and dry deposition of sulfur in Northern China

Y. P. Pan et al.

Title Page

Abstract | Introduction

Conclusions | References

Tables | Figures

◄ | ►|

◄ | ►

Back | Close

Full Screen / Esc

Printer-friendly Version

Interactive Discussion

Wang, Y., Yu, W., Pan, Y., and Wu, D.: Acid neutralization of precipitation in Northern China, J. Air. Waste. Manage., 62, 204–211, doi:10.1080/10473289.2011.640761, 2012.

Wesely, M. L.: Parameterization of surface resistances to gaseous dry deposition in regional-scale numerical models, Atmos. Environ., 23, 1293–1304, doi:10.1016/0004-6981(89)90153-4, 1989.

Wesely, M. L. and Hicks, B. B.: A review of the current status of knowledge on dry deposition, Atmos. Environ., 34, 2261–2282, doi:10.1016/s1352-2310(99)00467-7, 2000.

Wu, D., Wang, Y. S., Pan, Y. P., Xin, J. Y., and Tang, G. Q.: Application of passive sampler to monitor and study atmospheric trace gases in Beijing-Tianjin-Hebei area, Environ. Sci., 31, 2844–2851, 2010 (in Chinese).

Wyers, G. P. and Duyzer, J. H.: Micrometeorological measurement of the dry deposition flux of sulphate and nitrate aerosols to coniferous forest, Atmos. Environ., 31, 333–343, doi:10.1016/S1352-2310(96)00188-4, 1997.

Yang, F., Tan, J., Shi, Z. B., Cai, Y., He, K., Ma, Y., Duan, F., Okuda, T., Tanaka, S., and Chen, G.: Five-year record of atmospheric precipitation chemistry in urban Beijing, China, Atmos. Chem. Phys., 12, 2025–2035, doi:10.5194/acp-12-2025-2012, 2012.

Zhang, Q., Streets, D. G., Carmichael, G. R., He, K. B., Huo, H., Kannari, A., Klimont, Z., Park, I. S., Reddy, S., Fu, J. S., Chen, D., Duan, L., Lei, Y., Wang, L. T., and Yao, Z. L.: Asian emissions in 2006 for the NASA INTEX-B mission, Atmos. Chem. Phys., 9, 5131–5153, doi:10.5194/acp-9-5131-2009, 2009.

Zhang, Y., Wu, S. Y., Krishnan, S., Wang, K., Queen, A., Aneja, V. P., and Arya, S. P.: Modeling agricultural air quality: current status, major challenges, and outlook, Atmos. Environ., 42, 3218–3237, doi:10.1016/j.atmosenv.2007.01.063, 2008.

Zhao, D., Xiong, J., Xu, Y., and Chan, W. H.: Acid rain in southwestern China, Atmos. Environ., 22, 349–358, doi:10.1016/0004-6981(88)90040-6, 1988.

Zhao, Y., Duan, L., Xing, J., Larssen, T., Nielsen, C. P., and Hao, J.: Soil acidification in China: is controlling SO_2 emissions enough?, Environ. Sci. Technol., 43, 8021–8026, doi:10.1021/es901430n, 2009.

Title Page

Abstract | Introduction

Conclusions | References

Tables | Figures

◄ | ►►

◄ | ►

Back | Close

Full Screen / Esc

Printer-friendly Version

Interactive Discussion
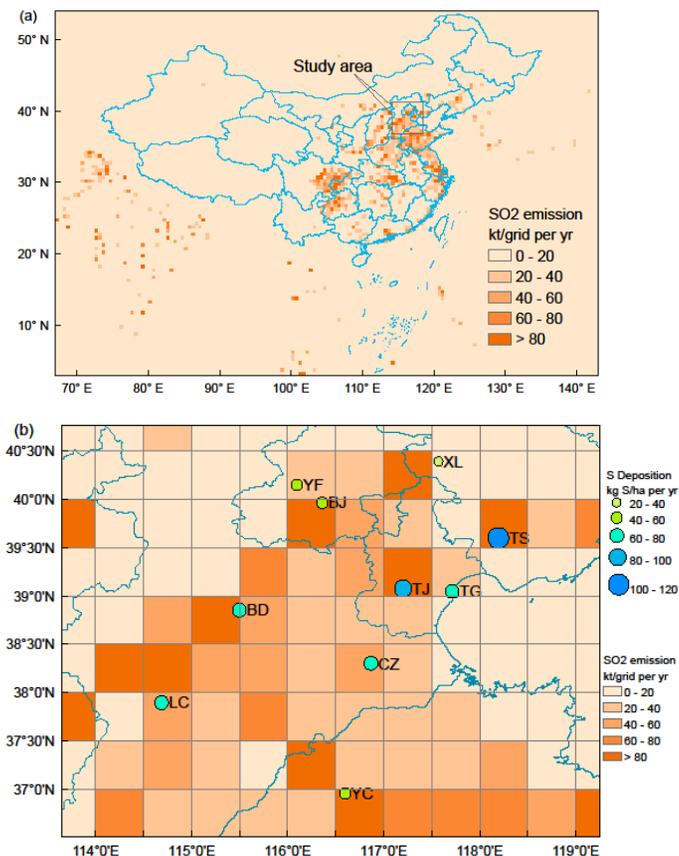
Fig. 1. Locations of the study area **(a)** and the sampling sites **(b)** in Northern China with SO$_2$ emission distributions. The total sulfur deposition data are means of 3-yr observations from December 2007 to November 2010. The emission data of SO$_2$ are from 2006 (Zhang et al., 2009), with a resolution of 30 min × 30 min. The definition of the site codes is found in Sect. 2.1.

Title Page

Abstract | Introduction

Conclusions | References

Tables | Figures

|◀ | ▶|

◀ | ▶

Back | Close

Full Screen / Esc

Printer-friendly Version

Interactive Discussion
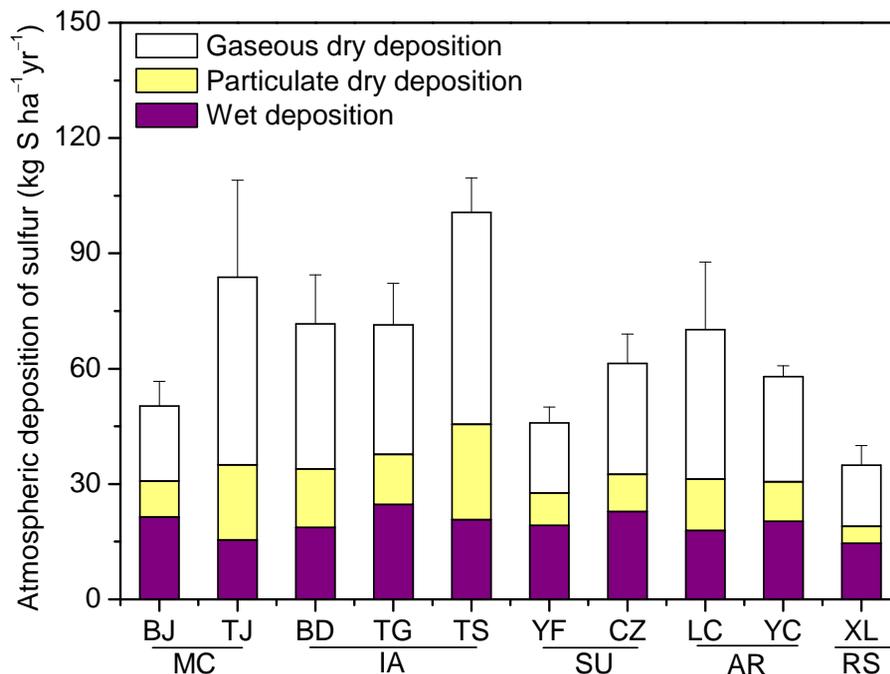
Fig. 2. Atmospheric deposition flux of sulfur via precipitation, particles and gases at the ten sites in Northern China. The data shown are means of 3-yr observations, with the error bars denoting standard deviation. MC, IA, SU, AR and RS denote urban, industrial, suburban, agricultural and rural sites, respectively. The definition of the site codes is found in Sect. 2.1.
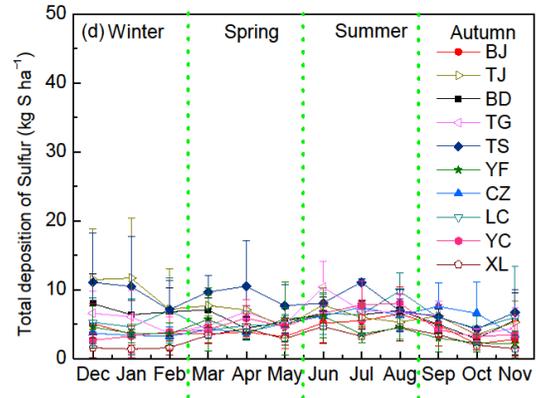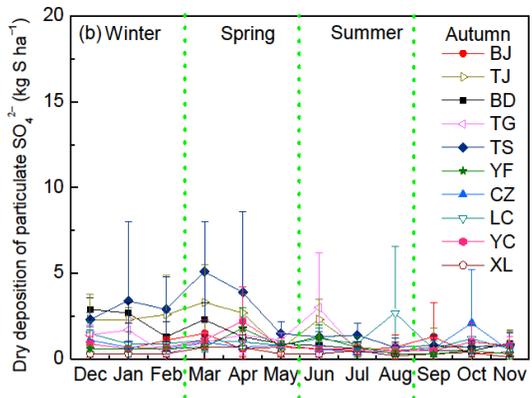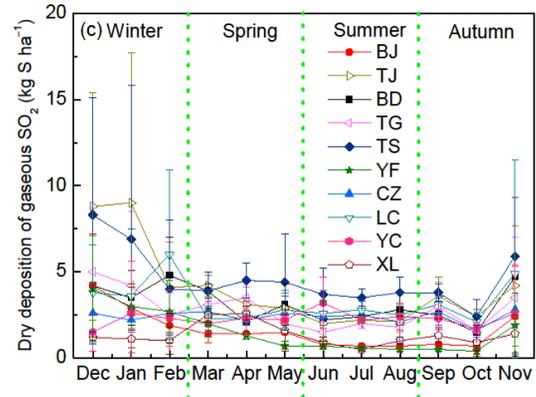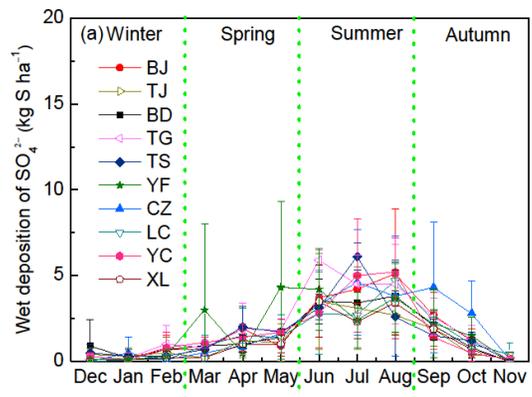
Fig. 3. Seasonal variations of the atmospheric deposition flux of sulfur at the ten selected sites in Northern China. The data shown are the monthly mean ± standard deviations of 3-yr observations (from December 2007 to November 2010). The definition of the site codes is found in Sect. 2.1.

Title Page

Abstract | Introduction

Conclusions | References

Tables | Figures

|◄ | ►|

◄ | ►

Back | Close

Full Screen / Esc

Printer-friendly Version

Interactive Discussion
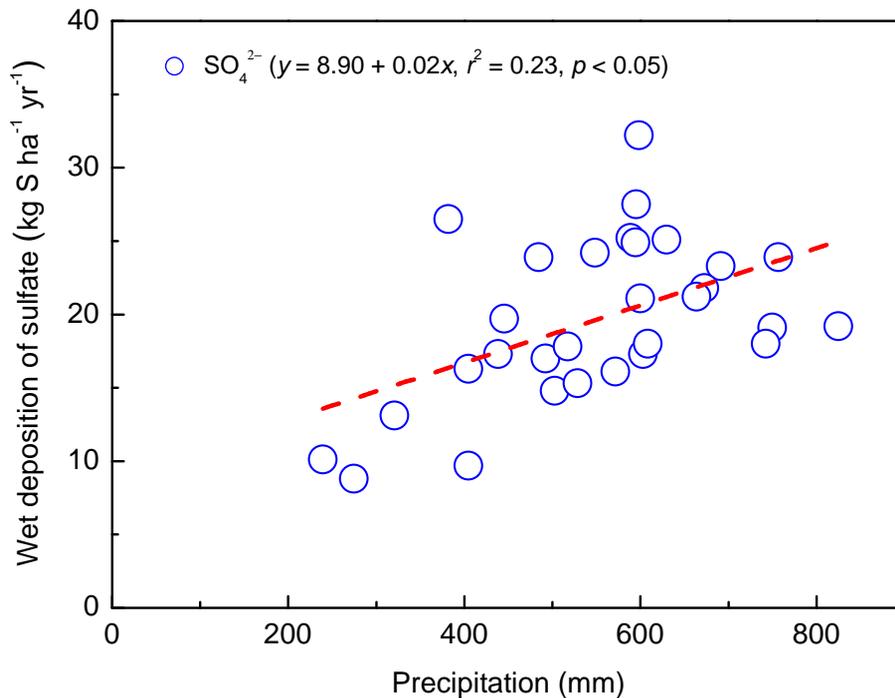
Fig. 4. Annual wet deposition flux of sulfur vs. precipitation amount at the ten selected sites in Northern China.

Title Page

Abstract | Introduction

Conclusions | References

Tables | Figures

◄◄ | ►►

◄ | ►

Back | Close

Full Screen / Esc

Printer-friendly Version

Interactive Discussion
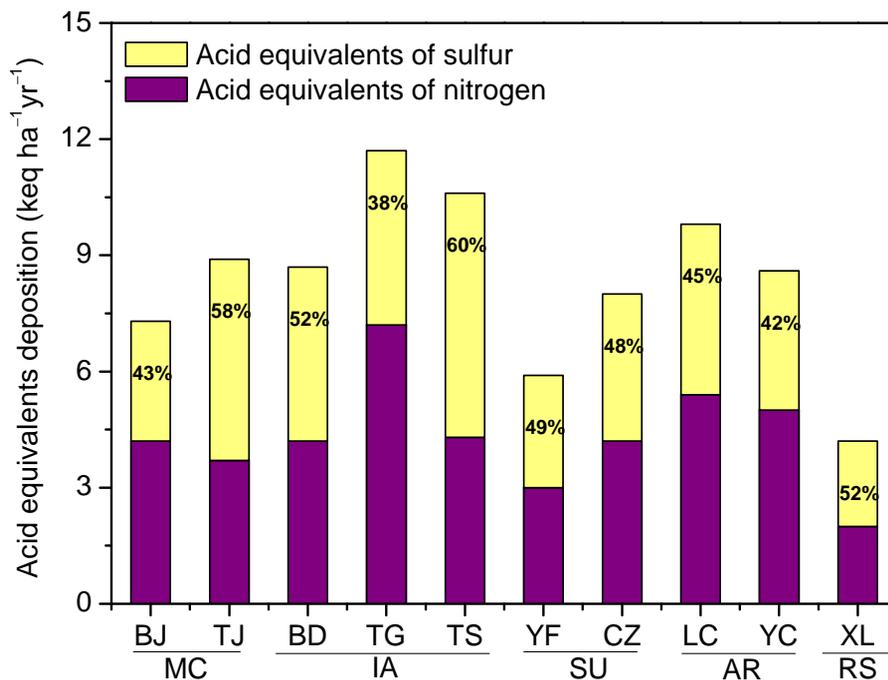
Fig. 5. Total "acid equivalents" deposition of sulfur and nitrogen at the ten selected sites in Northern China. The data shown are means of 3-yr observations. MC, IA, SU, AR and RS denote urban, industrial, suburban, agricultural and rural sites, respectively. Percentage in each bar represents the proportion of sulfur contribution to acid equivalent deposition at the corresponding site. The definition of the site codes is found in Sect. 2.1.